Coevolutionary dynamics on scale-free networks

Sungmin Lee and Yup Kim*
Department of Physics and Research Institute for Basic Sciences, Kyung Hee University, Seoul 130-701, Korea
(Received 22 November 2004; published 19 May 2005)

We investigate Bak-Sneppen coevolution models on scale-free networks with various degree exponents γ including random networks. For $\gamma > 3$, the critical fitness value f_c approaches a nonzero finite value in the limit $N \to \infty$, whereas f_c approaches zero as $2 < \gamma \leqslant 3$. These results are explained by showing analytically $f_c(N) \simeq A/\langle (k+1)^2 \rangle_N$ on the networks with size N. The avalanche size distribution $P(s)$ shows the normal power-law behavior for $\gamma > 3$. In contrast, $P(s)$ for $2 < \gamma \leqslant 3$ has two power-law regimes. One is a short regime for small s with a large exponent τ_1 and the other is a long regime for large s with a small exponent τ_2 ($\tau_1 > \tau_2$). The origin of the two power regimes is explained by the dynamics on an artificially made star-linked network.

DOI: 10.1103/PhysRevE.71.057102 PACS number(s): 05.65.+b, 87.23.−n, 05.40.−a, 87.10.+e

Bak and Sneppen (BS) [1] have introduced an excellent model to explain the evolution of biospecies, which exhibits the *punctuated equilibrium* behavior [2]. The BS model has two important features, namely, coevolution of the interacting species and the intermittent bursts of activity separating relatively long periods of the stasis. In the BS model, the ecosystem evolves into a self-organized criticality with avalanches of mutations occurring on all scales. Aside from its importance for the evolution, the BS model has been also shown to have rich scaling behaviors [3].

Since the BS model was suggested, the model has been extensively studied on regular lattices or networks [3]. However, many important biosystems have been elucidated to form nontrivial networks by the recently developed network theories [4]. Important examples are the metabolic network, the cellular network, and the protein network [5–8]. Some of the most important bionetworks are scale-free networks (SFNs) [4], in which the degree distribution $p(k)$ satisfies a power law $p(k) \sim k^{-\gamma}$ [4]. Thus it is important to study the BS dynamics on SFNs or to find out how the base structure of interacting biological elements (cells, proteins, or species) affects the evolutionary change or dynamics of the given biosystem. Until now, BS models on the nontrivial networks were not investigated extensively. Christensen *et al.* [9] have studied the BS model on random networks (RNs). Kulkani *et al.* [11] studied the BS model on small-world networks. Slanina and Kotrla [12] studied the forward avalanches of a sort of extremal dynamics with evolving networks. Moreno and Vazquez [13] studied the BS model only on a SFN with $\gamma = 3$.

In this paper, we will study BS models on SFNs in complete and comprehensive ways. One of the main purposes of this study is to find which structure of interacting species is the most stable network or the closest to a mutation-free network under the coevolationary change with interacting species. As is well known, SFNs with the degree exponent $2 < \gamma \leqslant 3$ are physically much different from those with $\gamma > 3$ [4]. We study BS models not only on SFNs with $2 < \gamma \leqslant 3$ but also on SFNs with $\gamma > 3$ including random networks (or SFNs with $\gamma = \infty$). As we shall see, two important results are found in this study. First, the critical fitness value f_c of BS models for $\gamma \leqslant 3$ is shown to have the limiting behavior $f_c(N) \to 0$ when the number of nodes N of the network goes to infinity. In contrast, f_c approaches a finite nonzero value as $N \to \infty$ for $\gamma > 3$. Furthermore, $f_c(N)$ on SFNs with finite N is shown to satisfy the relation $f_c(N) \simeq \mathrm{const}/\langle (k+1)^2 \rangle_N$, which is also directly supported by simulation. Second, for $2 < \gamma \leqslant 3$ the distribution of avalanches is shown to have two power-law regimes. To find the origin of this anomalous behavior of avalanches, we also study BS models on an artificially made star-linked network and find the two similar power-law regimes.

We now explain the model treated in this paper. All the models are defined on a graph $Gr = \{N, K\}$, where N is the number of nodes and K is the number of degrees with the average degree $\langle k \rangle = 2K/N$. Initially, a random fitness value $f_i \in [0,1]$ is assigned to each node $i = 1, \ldots, N$. At each time step, the system is updated by the following two rules. (i) First, assign a new fitness value to the node with the smallest fitness value $f_{\min}$. (ii) Second, assign new fitness values to the nodes which are directly connected to the node with $f_{\min}$. We use SFNs with the various degree exponents γ as $Gr = \{N, K\}$. To generate SFNs, we use the static model [14] instead of the preferential attachment algorithm [4].

To understand the dependence of the critical fitness value $f_c(N)$ on γ, we generate SFNs with $\gamma = \infty$, $5.7 \sim 2.15$. To exclude the effects of finite percolation clusters [9] and to see the effect of the network structure itself, all the networks are made to have an average degree $\langle k \rangle = 4$. To understand the dependence on the number of nodes N, the networks with the sizes $N = 10^3 - 10^6$ are generated for each γ. To determine the critical fitness value $f_c(N)$, we consider $f_{\min}$ as a function of the total number of updates s [3]. Initially, $f_{\min}(s=0)$ is the gap $G(0)$, where $G(s)$ is the maximum of all $f_{\min}(s')$ for $0 \leqslant s' \leqslant s$ [3]. When $G(s)$ jumps to a new higher value, there are no nodes in the system with $f_i(s) < G(s)$. Thus $\lim_{s \to \infty} G_N(s) = f_c(N)$.

We measure $f_c(N)$ on the various SFNs. Figure 1 shows the plot of $f_c(N)$ vs $1/N$ for SFNs with various γ. The values of critical fitness $f_c(N \to \infty)$ evaluated from data in Fig. 1 are 0.21(1), 0.19(1), 0.15(1), and 0.09(1) for $\gamma = \infty$, 5.7, 4.3, and

*Electronic address: ykim@khu.ac.kr

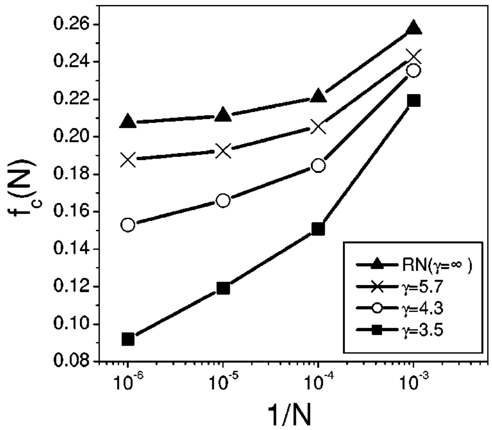

FIG. 1. Semilog plot of the threshold $f_c(N)$ vs $1/N$ on RN and on SFNs with $\gamma=5.7$, 4.3, and 3.5. Used network sizes are $N=10^3, 10^4, 10^5$, and 10^6. The solid lines between data points are obtained by simple linear interpolations.

3.5. The results in Fig. 1 mean that for $\gamma>3$, $f_c(N\to\infty)\to\mathrm{const}(>0)$.

Figure 2 shows the plot of $f_c(N)$ vs $1/N$ for $2<\gamma\leqslant 3$. For $\gamma=3$, $f_c(N)$ nicely satisfies the relation $f_c(N)\sim 1/\ln N$ [13]. For $2<\gamma<3$, $f_c(N)$'s seem to follow a power law $f_c(N)\sim N^{-\eta}$ and approach to zero as N goes to ∞. In contrast to the results in Fig. 1, $f_c\to 0$ for $2<\gamma\leqslant 3$.

In the RN, every pair of nodes is randomly connected and the degree distribution is a Poisson distribution [4,9]. So the BS model on RN [9] is a good realization of the mean-field-type random neighbor model. In the random neighbor model, the fitness values of the randomly selected $(m-1)$ nodes as well as the node with $f_{\min}$ are updated and $f_c=1/m$ [10]. The result $f_c(\infty)=0.21$ (1) on RN is very close to $1/(\langle k\rangle+1)=\frac{1}{5}$, which is expected from the random neighbor model by setting $\langle k\rangle+1=m$ [9]. In the steady state of the BS model, the probability measure $P(f<f_c)$ is 0. Consider the case in which the number of updates for each step is fixed as m, as in the random neighbor model. To sustain the steady state in this case, at most one new fitness value should be less than f_c and the other $m-1$ new values should be larger than f_c [10]. Therefore, we can easily see $mf_c=1$ or $f_c=1/m$.

On a network, the number of updates depends on the degree of the node with $f_{\min}$, and the probability which a node with degree k is connected to the node with $f_{\min}$ should be proportional to k. For an updating step, the probability that a node with degree k is updated is proportional to $k+1$, because the node itself can be the node with $f_{\min}$. Therefore, after an arbitrary update, the probability $P_{\min}(k)$ of a node with degree k being the node with $f_{\min}$ is proportional to $k+1$. This means that $P_{\min}(k)$ in the steady state should be proportional to $k+1$, or

$$P_{\min}(k)=\frac{(k+1)p(k)}{\sum_k (k+1)p(k)}=\frac{1}{\langle k\rangle+1}(k+1)p(k).$$

The average number N_{update} of the nodes updated for one updating process is therefore

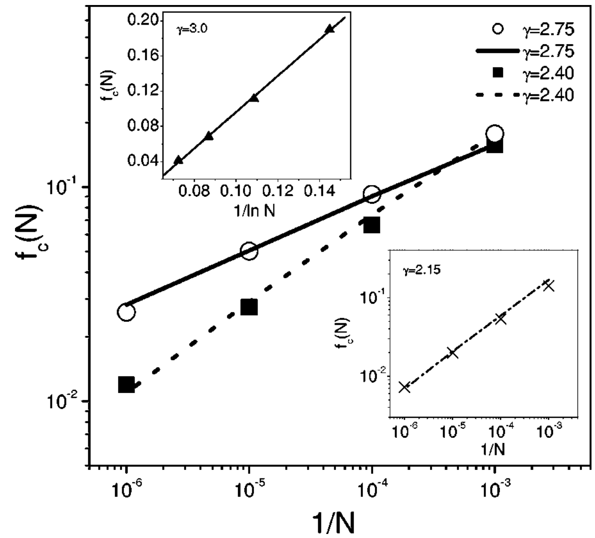

FIG. 2. Log-log plot of $f_c(N)$ and $A/\langle k(N)^2\rangle_N$ vs $1/N$ on SFNs with $\gamma=2.75$, 2.40, and 2.15. Symbols are for $f_c(N)$ and the lines are for $A/\langle k(N)^2\rangle_N$, where A is a constant. The top inset shows the plot of $f_c(N)$ vs $1/\ln N$ for $\gamma=3.0$.

$$N_{\text{update}}=\sum_k (k+1)P_{\min}(k)=\frac{\sum_k (k+1)^2 p(k)}{\langle k\rangle+1} \tag{1}$$

and thus f_c is

$$f_c=\frac{1}{N_{\text{update}}}=\frac{\langle k\rangle+1}{\sum_k (k+1)^2 p(k)}=\frac{\langle k\rangle+1}{\langle (k+1)^2\rangle}. \tag{2}$$

When the number of updates is fixed as m, Eq. (2) reproduces the mean-field result $f_c=1/m$. In SFNs with $p(k)\simeq k^{-\gamma}$, Eq. (2) becomes

$$f_c\simeq\begin{cases}\text{finite}, & \gamma>3\\ \dfrac{A}{\langle k^2\rangle}=\dfrac{A}{\displaystyle\int k^{2-\gamma}dk}, & 2<\gamma\leqslant 3.\end{cases} \tag{3}$$

Equation (3) explains the results in Figs. 1 and 2, including the result $f_c\simeq 1/\ln N$ for $\gamma=3$. For $2<\gamma<3$, measured $f_c(N)$ is fitted to the relation $f_c(N)=A/\langle k^2\rangle_N$, where A is constant and $\langle k^2\rangle_N$ is $\langle k^2\rangle$ for the network with the size N. The fitted lines in Fig. 2 show that the relation $f_c(N)=A/\langle k^2\rangle_N$ holds well and directly supports Eq. (3).

An avalanche in the Bak-Sneppen model is defined as the sequential step s for which the minimal site has a fitness value smaller than given f_o [3]. For each network, we choose f_o to satisfy $[f_c(N)-f_o]/f_c(N)=0.05$. The probability distribution $P(s)$ of avalanche size s on the networks with the size $N=10^6$ is shown in Figs. 3 and 4. All the data in Figs. 3 and 4 are taken in the steady states.

As is shown in Fig. 3, $P(s)$ in SFNs with $\gamma>3$ including RN satisfy the normal power-law behavior with an exponential cutoff as $P(s)=As^{-\tau}\exp(-s/s_c)$. The curves in Fig. 3 represent the fitted curves to data for $P(s)$. From those fit-

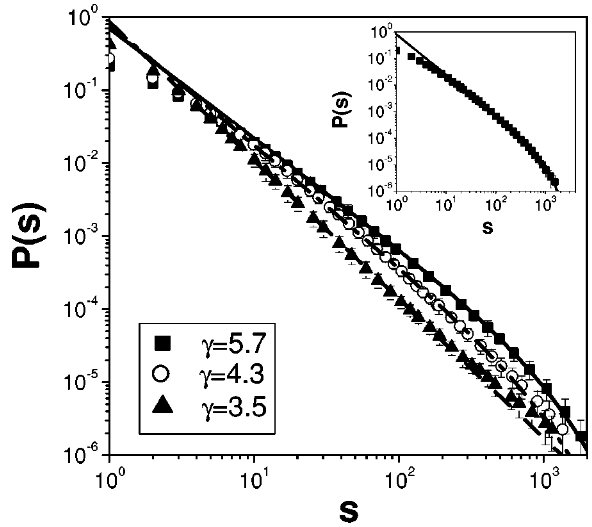

FIG. 3. Log-log plot of the avalanche size distribution $P(s)$ on SFNs with $\gamma=5.7$, $\gamma=4.3$, $\gamma=3.5$, and on RN (Inset). The curves for $\gamma=5.7$, $\gamma=4.3$, and RN denote the fits of the form $P(s) = As^{-\tau}\exp(-s/s_c)$ to the data. Obtained exponents are $\tau=1.5$ for both $\gamma=5.7$ and RN, and $\tau=1.65$ for $\gamma=4.5$. The line for $\gamma=3.5$ denotes the fit of the form $P(s)=As^{-\tau}$ $(\tau=1.65)$ without cutoff.

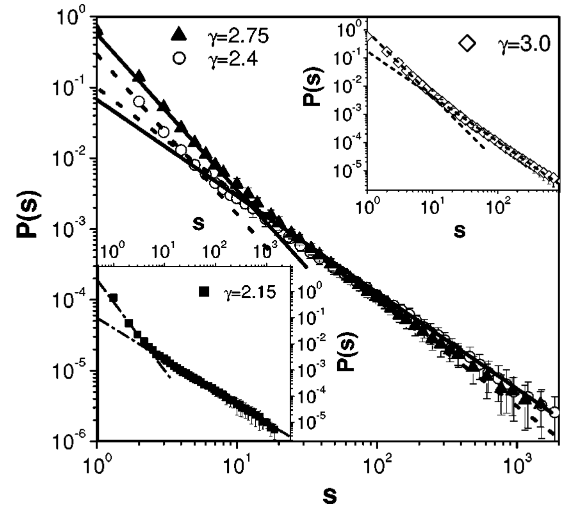

FIG. 4. Log-log plot of $P(s)$ on SFNs with $\gamma=3$ (top inset), 2.75, 2.4, and 2.15. Two crossing lines for each data set denote the two power-law regimes, $P(s)=As^{-\tau_1}$ and $P(S)=Bs^{-\tau_2}$. Obtained exponents, τ_1 and τ_2, are shown in Table I.

tings, the obtained values for τ are 1.5 for RN and $\gamma=5.7$, and 1.65 for $\gamma=4.3$. The result for RN and SFN with $\gamma=5.7$ is expected from the random neighbor model [10]. As γ decreases to 4.0 or so, τ increases to 1.65. For $\gamma=3.5$, however, the best fitting function is $P(s)=Bs^{-\tau}$ with $\tau=1.65$ and we cannot find the cutoff-dependent behavior within our data. Instead, it is even observed that tails of measured data for $\gamma=3.5$ around $s=10^3$ seem to deviate from the fitting function $P(s)=Bs^{-\tau}$ and are larger than values estimated from the best fitting function. This rather anomalous tail behavior of $P(s)$ for $\gamma=3.5$ should be the signal of the anomalous behavior of $P(s)$ for $2<\gamma\leqslant 3$.

In contrast to the simple power-law behavior for $\gamma>3$, anomalous behavior for $P(s)$ shows up for $2<\gamma\leqslant 3$ (Fig. 4). We can see two power-law regimes clearly for $P(s)$ in Fig. 4. Initially, the avalanche size distribution follows $P(s)\simeq s^{-\tau_1}$ about 1 decade or so. After this short initial power-law regime, the long second power-law regime appears as $P(s) \simeq s^{-\tau_2}$, where $\tau_1>\tau_2$. The measured exponents τ_1, τ_2 are summarized in Table I.

Compared to the behavior of the avalanche size distribution for $\gamma>3$, this anomalous behavior of $P(s)$ is very peculiar. In the steady state, it is expected that the node with $f_{\min}$ (the minimal node) is most frequently found among the last updated nodes [10] and then the minimal node locally performs a random walk. However, there can be longer jumps of any length with a very low probability. If this kind of a *jumpy random walk* is the motion of the minimal node, then a subnetwork consists of a *hub node* (*center node*) and many *slave nodes* directly linked to the hub should be important to decide the behavior of $P(s)$. Due to the *jumpy random walk* behavior, the more slave nodes the hub node has, the longer is the stay of the minimal node or the longer the avalanche exists at the given subnetwork. This effect explains the second power-law regime with the exponent τ_2 in Fig. 4, because $\langle k^2\rangle$ diverges for $2<\gamma\leqslant 3$, and so the subnetwork of a hub node and many slave nodes should be the main substructure in SFNs with $2<\gamma\leqslant 3$. Evidently, the jumpy steps of the *jumpy random walk* make the shorter avalanches possible and this effect explains the first power-law regime with the exponent τ_1.

To support the qualitative explanation of the two power-law regimes, we consider an artificially made star-linked network shown in Fig. 5. In the star-linked network, a main subnetwork consists of a center (star) node and many dangling slave nodes linked directly to the star node. Then the center nodes are linked hierarchically to one after another as sketched in Fig. 5(a). We make a star-linked network in which there are 25 base subnetworks with 500, 480, …, and 20 slave nodes, respectively. In this network, we perform BS dynamics and find $f_c=0.123$. $P(s)$ is also measured on the star-linked network and is shown in Fig. 5(b). We find the two power-law regimes with the exponents $\tau_1=3.7$ and $\tau_2=1.27$. The plateau between two power regimes in the data of $P(s)$ in Fig. 5(b) is probably from the discrete distribution of the number of slave nodes.

In conclusion, we study BS models on SFNs with various γ. For $\gamma>3$, f_c approaches a nonzero value in the limit $N\to\infty$ and $P(s)$ shows normal power-law behavior with $\tau \geqslant 1.5$. For $\gamma\leqslant 3$, f_c approaches zero as $f_c(N)\simeq A/\langle K^2\rangle_N$ and

TABLE I. Two power-law exponents, τ_1 and τ_2, for SFNs with $\gamma\leqslant 3$.

γ	τ_1	τ_2
3.0	2.09	1.59
2.75	2.22	1.47
2.4	2.27	1.32
2.15	2.30	1.20

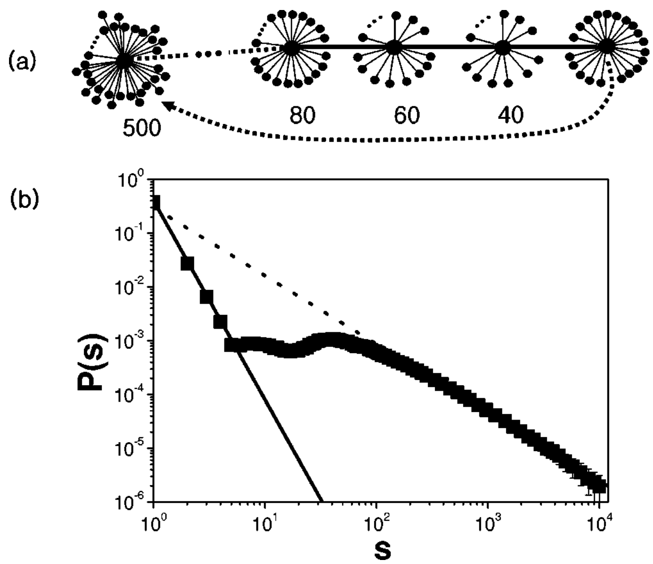

FIG. 5. (a) Schematic of a star-linked network which consists of 25 subnetworks with 500, 480, …, and 20 dangling slave nodes. (b) Plot of $P(s)$ on the star-linked network structure. Two power-law regimes with $P(s)=As^{-\tau_1}(\tau_1=3.7)$ and $P(s)=Bs^{-\tau_2}$ $(\tau_2=1.27)$ are clearly shown by the lines.

$P(s)$ has two power-law regimes. The origin of the two power regimes is explained by the dynamics on a star-linked network.

In Ref. [13], BS dynamics only on a SFN with $\gamma=3$ was studied and the only meaningful numerical result was to show $f_c(N)\simeq 1/\ln N$. Reference [13] suggested a relation similar to Eq. (2) from a rate equation which was obtained by a naive and immature analogy of BS dynamics to the epidemic dynamics on SFNs [15]. However, the rate equation should never be the exact one. Even the exact rate equation for the simple random neighbor model [10] is much more complex than that of Ref. [13] or the epidemic dynamics. The correct rate equation for BS dynamics on SFNs must be derived by considering all the terms of the rate equation in Ref. [10] and the base network structure simultaneously and correctly. The derivation of the correct rate equation should be a subject for future study. In Ref. [13], it was argued that $P(s)$ for $\gamma=3$ satisfies a simple power law with $\tau\simeq 1.55$. By the brute-forced fit of the relation $P(s)\simeq s^{-\tau}$ to our data in Fig. 4, we also obtain $\tau\simeq 1.6$ for $\gamma=3$. However, this blind application of the simple power law should be wrong and there should exist the two-power law regimes even for $\gamma=3$. One can easily identify the two power-law regimes in the $P(s)$ data of Ref. [13] rather clearly, although the tail parts of their data are qualitatively poor and show large fluctuations.

The occurrence of two power-law regimes for $P(s)$ was also found in BS dynamics on small-world networks [11] and in an extremal dynamics with evolving networks [12]. However the origins of the two power-law regimes were completely different from ours. The origin in the small-world networks was argued to be the long-range connectivity of the networks [11]. The extremal dynamics with evolving random networks [12] changes the network structure and is not exactly the same as BS dynamics. Furthermore, the evolving network develops many disconnected clusters. In the model [12], the forward avalanches are mainly measured. The forward avalanches [12] should be affected by the dynamical aggregation and splitting of subnetworks by the extremal dynamics, which should be the origin of the two power-law regimes. In contrast, our avalanches of BS dynamics are measured on a fully connected static scale-free network and should not be directly comparable to the avalanches on dynamically varying networks.

The authors would like to thank Professor H. Jeong for valuable suggestions. This work is supported by Korea Research Foundation Grant No. KRF-2004-015-C00185.

[1] P. Bak and K. Sneppen, Phys. Rev. Lett. **71**, 4083 (1993).
[2] S. A. Kauffman and S. J. Johnsen, J. Theor. Biol. **149**, 467 (1991).
[3] M. Paczuski, S. Maslov, and P. Bak, Phys. Rev. E **53**, 414 (1996).
[4] R. Albert and A.-L. Barabási, Rev. Mod. Phys. **74**, 47 (2002); S. N. Dorogovtsev and J. F. F. Mendes, Adv. Phys. **51**, 1079 (2002).
[5] H. Jeong, B. Tomber, R. Albert, Z. N. Oltvai, and A.-L. Barabási, Nature (London) **407**, 651 (2000).
[6] H. Jeong, S. Mason, A.-L. Barabási, and Z. N. Oltvai, Nature (London) **411**, 41 (2001).
[7] R. J. Williams and N. D. Martinez, Nature (London) **404**, 180 (2000).
[8] J. Camacho, R. Guimerà, and L. A. N. Amaral, Phys. Rev. E **65**, 030901(R) (2002).
[9] K. Christensen, R. Donangelo, B. Koiller, and K. Sneppen, Phys. Rev. Lett. **81**, 2380 (1998).
[10] H. Flyvbjerg, K. Sneppen, and P. Bak, Phys. Rev. Lett. **71**, 4087 (1993).
[11] R. V. Kulkarni, E. Almaas, and D. Stroud, e-print cond-mat/9905066.
[12] F. Slanina and M. Kotrla, Phys. Rev. Lett. **83**, 5587 (1999); Phys. Rev. E **62**, 6170 (2000).
[13] Y. Moreno and A. Vazquez, Europhys. Lett. **57**, 765 (2002).
[14] K.-I. Goh, B. Kahng, and D. Kim, Phys. Rev. Lett. **87**, 278701 (2001).
[15] R. Pastor-Satorras and A. Vespignani, Phys. Rev. Lett. **86**, 3200 (2001); Phys. Rev. E **63**, 066117 (2001).